From Public-Demo Incident to Bystander-Safety Contract: A Cross-Standards Framework for Speed-and-Separation and Power-and-Force Requirement Derivation in Untethered Humanoid Robots

Jherrod Thomas
Independent Researcher — *The Lion of Functional Safety*
jherrodthomas.com June 2026

***Abstract*—A cluster of bystander-contact events involving untethered humanoid robots in public performances during the first half of 2026—most prominently a Unitree G1 that executed a scripted roundhouse kick and struck a child at a botanical-garden demonstration in Urumqi, China, on 1 June 2026—exposes a structural gap in current robotic-safety practice. The machines did not malfunction; they executed their choreography within specification, in a deployment context for which no risk assessment, separation calculation, or contact-force budget had been performed. The governing standards each address part of the problem: ISO 10218-1/-2:2025 and ISO/TS 15066:2016 define the collaborative control vocabulary but scope themselves to industrial robots; ISO 13855:2024 supplies the separation-distance methodology but assumes a guarded machine; ISO 13482:2014 addresses personal-care robots but omits the bystander and crowd hazards specific to public space; and ISO/CD 25785-1 for dynamically stable mobile robots is not yet published. No single instrument closes the loop from a contact incident to a verifiable, mode-gated requirement. We propose a six-step framework that ingests incident evidence, characterizes the reachable kinematic envelope, allocates ISO/TS 15066 biomechanical contact limits, computes an ISO 13855 protective separation distance, derives a mode-gated behavior policy with a minimum-risk condition, and allocates a protective-stop performance level per ISO 13849-1. We provide two numbered equations—a separation-distance contract and a transient-contact-force constraint—one framework figure, one fault tree, and two tables. We demonstrate the framework on the Unitree G1 demonstration cluster and derive five traceable requirements.**

***Index Terms*—ISO/TS 15066, ISO 10218-2, ISO 13855, ISO 13482, humanoid robot, speed and separation monitoring, power and force limiting, minimum risk condition, performance level.**

I. Introduction

The deployment of untethered, full-size humanoid robots into public and semi-public environments accelerated sharply through 2025 and into 2026, driven by production volumes that were until recently confined to research laboratories. Several Chinese manufacturers now report annual humanoid output in the thousands of units, and public demonstrations—choreographed dance, martial-arts routines, greeting and interaction shows—have become the dominant marketing channel for the category [3]. These demonstrations place torque-dense, dynamically balanced bipedal machines among untrained crowds at separation distances approaching zero, frequently with children present by design.

A cluster of bystander-contact events in the first half of 2026 makes the resulting hazard concrete rather than hypothetical. On 1 June 2026, at the Urumqi Botanical Garden in China's Xinjiang region, a Unitree G1 humanoid performing a scripted martial-arts routine executed a spinning roundhouse kick and struck a young child in the abdomen; handlers reacted only after contact [1]. Earlier in 2026, a separate G1 lost its balance during a live performance, fell, and—while grounded—struck a nearby adult with uncontrolled limb motion, fracturing the man's nose [1]. On 24 April 2026, at a university event in Xi'an, a humanoid in a dance routine deviated from its program, reportedly under radio-frequency interference, and grasped a student; the event was logged by the OECD AI Incidents Monitor [2].

The popular framing—*robot goes rogue*—inverts the engineering reality. In at least the Urumqi case the robot did not malfunction: it executed its programmed choreography correctly. The child was simply inside the performance envelope, and nothing in the deployment was designed to notice or to intervene. The three events share three distinct proximate causes—a scripted motion intersecting an intruding bystander, a post-fall absence of joint-torque suppression, and a corrupted control input—but a safety engineer should read them as a single hazard, *bystander struck during public humanoid performance*, reached through three independent branches of one fault tree that was never drawn.

The standards landscape brackets this gap tightly but does not close it. ISO 10218-1:2025 and ISO 10218-2:2025 define the safety vocabulary of safeguarded space, speed-and-separation monitoring, and power-and-force limiting [4], [5], and ISO/TS 15066:2016 supplies the biomechanical contact-limit tables that power-and-force limiting must respect [6]. But these instruments scope themselves to *industrial* robots. ISO 13855:2024 provides the separation-distance methodology any speed-and-separation argument depends on, yet it assumes a guarded, fixed machine with a detection device [7]. ISO 13482:2014 is the nearest in-scope product standard for a robot among the public, yet recent analysis shows it omits the bystander, crowd, and proxemic hazards that define public space [8], [25]. ISO 12100:2010 obliges the manufacturer to consider reasonably foreseeable misuse—of which a child approaching an interesting machine is the paradigmatic case [9]—but it is a generic methodology, not an allocation. The first standard written specifically for dynamically stable legged machines, ISO/CD 25785-1, remains a committee draft as of mid-2026 [11].

The contribution of this paper is a method that closes the loop. First, we propose a six-step cross-standards framework that ingests public-record incident evidence and produces verifiable, mode-gated bystander-safety requirements with an allocated protective-stop performance level. Second, we formalize two contracts as numbered equations: an ISO/TS 15066 transient-contact-force constraint used to prove that strike-class motions cannot be made power-and-force compliant and an ISO 13855-style protective separation distance specialized to a striking envelope. Third, we demonstrate the framework end-to-end on the 2026 Unitree G1 demonstration cluster, producing a fault tree, a requirements table with performance-level allocation, and five traceable derived requirements. We are deliberate about what the framework cannot do: it converts a deterministic safeguarding problem into requirements, but it does not certify the learned, possibly non-deterministic behavior policies that increasingly drive these machines, and it does not address the social and proxemic dimensions of public-space safety.

II. Background and Related Work

A. Physical Human-Robot Interaction Safety

The foundations of physical human-robot interaction (pHRI) safety were laid in the mid-2000s. De Santis *et al.* compiled an atlas of pHRI organized around injury avoidance and useful interaction [13], and Bicchi and Tonietti argued that intrinsically compliant actuation could decouple the safety-versus-performance trade-off by limiting transferable energy at the hardware level [14]. The dominant control-side response is the collision detection, isolation, and reaction pipeline surveyed by Haddadin, De Luca, and Albu-Schäffer, who quantify the contact forces achievable under various reaction strategies [12]. This establishes a central premise: contact detection and reaction are mature, but they are necessary, not sufficient—a detected contact during a deliberately accelerated strike is already an injury.

B. The Four Collaborative Methods and ISO/TS 15066

ISO/TS 15066:2016 defines four collaborative operation methods: safety-rated monitored stop, hand guiding, speed-and-separation monitoring (SSM), and power-and-force limiting (PFL) [6]. SSM maintains a minimum protective separation distance and reduces robot speed as the distance closes; PFL bounds the robot so any contact stays below a biomechanical limit specific to the body region at risk. The specification tabulates quasi-static and transient force and pressure limits for 29 body locations; the abdominal region, for example, carries a quasi-static force limit of 110 N and a transient limit of twice that value [6]. Critically, Behrens *et al.* demonstrated through a 112-subject human-trial study that the ISO/TS 15066 limits are largely preliminary and that pain thresholds differ significantly by body region and by sex—a result that constrains how confidently any PFL argument can be made for a heterogeneous public that includes children [19]. Reviews of ISO/TS 15066 hazard analysis further show that conformance to the limit tables does not by itself guarantee safety for heavier or faster machines [20].

C. Speed-and-Separation Monitoring

The SSM minimum-protective-distance methodology derives from the safeguard-positioning logic of ISO 13855 [7]. Marvel and Norcross provided the canonical treatment of implementing SSM in collaborative workcells, analyzing the protective-distance equation, its inputs, and the latency budget an external observer system must meet [15]. Byner, Matthias, and Ding extended static SSM to a *dynamic* formulation in which the permissible robot velocity is computed online as a function of both separation distance and direction of motion [16]. Recent work pushes SSM toward richer perception—robust safety zones under uncertain dynamics [21], adaptive zone-switching, and binocular- and depth-vision human tracking [26]—and Lucci *et al.* showed that SSM and PFL can be combined in a single controller [17]. Zanchettin *et al.* formalized the safety metrics and control laws underlying collaborative cells [18]. The common assumption is a known, instrumented workspace; none of it addresses a free-roaming biped in an uninstrumented public garden.

D. Humanoid Fall Control and Legged-Machine Stability

A dynamically balanced biped that loses stability does not become inert on contact with the ground: its controller continues to command joint torques unless explicitly told to stop. Subburaman *et al.* survey the control of humanoid fall-over and organize the field into fall prediction, avoidance, and damage-minimizing strategies [23]. Li *et al.* present a minimized-falling-damage method that reshapes the impact posture to reduce peak forces [24]. This work targets damage to the *robot*; the complementary case—protecting a *bystander* within the fallen machine's reach radius while its actuators are still energized—is the gap the nose-fracture incident [1] exposes and that ISO/CD 25785-1 is being written to address [11].

E. Public Space, Service Robots, and the Standards Gap

Salvini, Paez-Granados, and Billard analyzed the safety of mobile robots in public spaces and identified concrete gaps in EN ISO 13482:2014, arguing that the standard implicitly assumes private-space hazards and lacks requirements to protect pedestrians and bystanders; they enumerate three properties of public space—crowds, social and proxemic norms, and human misbehavior—that current standards do not capture [25].

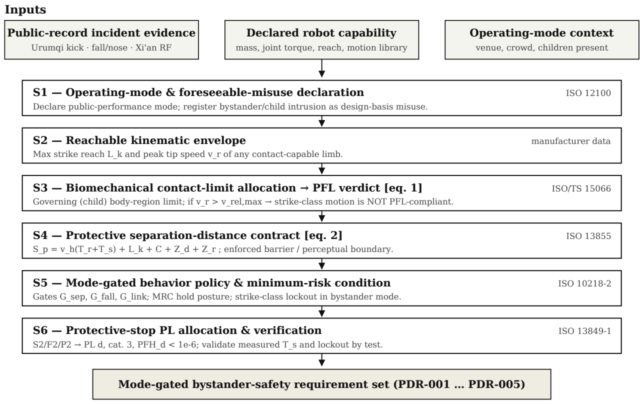

Fig. 1. Cross-standards framework. Incident evidence and declared robot capabilities (top) flow through six numbered stages (S1–S6) into ISO/TS 15066, ISO 13855, ISO 13849-1, and ISO 10218-2-compatible outputs (bottom). Each stage is annotated with its governing clause.

Safety-barrier-function and control-barrier-function methods offer a formal, run-time route to enforce separation and velocity constraints [22], and provide a candidate enforcement mechanism for the behavior-policy gates we derive. What the literature lacks, and what this paper supplies, is a structured translation from a specific public-demonstration contact incident to an allocated, verifiable requirement set keyed to the operating mode in which it occurred.

III. Approach: A Six-Step Framework

We propose a six-step framework, sketched in Fig. 1, that ingests public-record incident evidence and declared capability and produces a mode-gated bystander-safety requirement set with an allocated protective-stop performance level. The framework treats *public performance* as a distinct operating mode demanding its own hazard analysis, separation contract, contact-force budget, and stop authority.

A. Step S1 — Operating-Mode and Foreseeable-Misuse Declaration

The first step declares the operating mode and enumerates, per ISO 12100 [9], the reasonably foreseeable misuse events specific to that mode. For public performance, the controlling misuse event is a bystander—most foreseeably a child—entering the performance envelope mid-routine. A public-performance risk assessment lacking a row for bystander intrusion is, by the standard's own logic, incomplete.

B. Step S2 — Reachable Kinematic Envelope Characterization

The second step characterizes the reachable kinematic envelope: the maximum reach L_k of any contact-capable limb and the peak tip speed v_r within that envelope. For a strike-class motion—a kick or punch deliberately accelerating a distal limb mass—v_r is large and L_k spans the full leg or arm. For the worked example, the G1's roughly 35 kg mass and joint torques exceeding 100 N·m define an envelope whose distal speed is far above any power-and-force-limited regime [1].

C. Step S3 — Biomechanical Contact-Limit Allocation

The third step allocates the ISO/TS 15066 biomechanical contact limits to the reachable body regions of the exposed population [6], [19]. Because public demonstrations expose children, the framework requires that the limit for the most vulnerable reachable region govern: a strike at adult-abdomen height arrives at chest-to-head height on a small child, so the chest, neck, and skull limits become controlling. The transient contact force is modeled, following the ISO/TS 15066 spring-mass treatment, as

$$F_t = v_{\mathrm{rel}}\sqrt{k\,\mu}, \qquad \mu = \left(m_h^{-1} + m_r^{-1}\right)^{-1}, \tag{1}$$

where v_{rel} is the relative speed at contact, k is the effective contact stiffness of the body region, and μ is the effective two-body reduced mass formed from the human body-region mass m_h and the effective robot mass m_r. Requiring $F_t \leq F_{\mathrm{lim}}$ yields a maximum admissible contact speed $v_{\mathrm{rel,max}} = F_{\mathrm{lim}}/\sqrt{k\mu}$. The decision rule is immediate: if the strike-class tip speed v_r from S2 exceeds $v_{\mathrm{rel,max}}$—which it does for any deliberate strike—the motion cannot be made PFL-compliant and must be lockout-excluded from any bystander-present mode.

D. Step S4 — Protective Separation-Distance Contract

When PFL is unavailable, the framework falls back to SSM and computes the minimum protective separation distance using an ISO 13855 / ISO/TS 15066 formulation specialized to a striking envelope [7], [15], [16]:

$$S_p = v_h\,(T_r + T_s) + L_k + C + Z_d + Z_r, \tag{2}$$

where v_h is the human approach speed (ISO 13855 prescribes 1.6 m/s for walking approach and 2.0 m/s for upper-limb motion [7]), T_r is the control-system reaction time from intrusion detection to stop command, T_s is the actuation and mechanical stopping time, L_k is the maximum kinematic reach from S2, C is an intrusion allowance, and Z_d, Z_r are position-uncertainty terms. The output is an enforced physical barrier offset, or an equivalently validated perception-gated boundary, set no smaller than S_p.

E. Step S5 — Mode-Gated Behavior Policy and Minimum-Risk Condition

The fifth step instantiates a behavior policy that gates motion on the conditions of S3 and S4 and defines the minimum-risk condition (MRC). The intrusion gate G_{sep} suspends all strike-class motion and transitions to a bounded-speed hold posture when a bystander is detected inside S_p. The fall gate G_{fall} suppresses commanded joint torque to a safe-flail limit upon fall detection. The integrity gate G_{link} transitions to the MRC on detected control-link degradation or command implausibility. Candidate enforcement mechanisms include safety-rated monitored stops [4], [5] and run-time control-barrier-function filters [22].

F. Step S6 — Protective-Stop Performance-Level Allocation and Verification

The sixth step allocates a performance level (PL) to the protective-stop function per ISO 13849-1 [10]. Following the severity, frequency-of-exposure, and possibility-of-avoidance risk graph, a strike-class hazard against a child (severe, often irreversible injury—S2) at a public demonstration (high frequency of exposure—F2) with limited possibility of avoidance (P2) places the protective-stop function at PL d, requiring a category-3 architecture with a probability of dangerous failure per hour ($\mathrm{PFH_d}$) in the 10^{-7} to 10^{-6} band [10]. Verification follows ISO 10218-2 integration practice [5]: the measured stop time T_s is validated by test, strike-class lockout is verified by inspection of the motion library, and the separation distance is validated against measured detection and stop performance before first public run.

IV. Worked Example: The Unitree G1 Demonstration Cluster

We apply the framework to the 2026 Unitree G1 public-demonstration cluster [1], [2]. The functional thread is *execute a scripted performance routine in a public venue with uncontrolled bystanders*. We treat three failure modes jointly: a strike-class motion intersecting an intruding bystander (Urumqi kick), post-fall uncontrolled limb motion (nose fracture), and corrupted control input driving unplanned contact (Xi'an interference).

A. S1 — Operating Mode and Misuse

The operating mode is *public martial-arts/dance performance, children present*. The controlling foreseeable-misuse event per ISO 12100 [9] is *child enters performance envelope during scripted routine*. We add *robot loses balance on uneven outdoor surface* and *shared-spectrum venue corrupts wireless control* as two further mode-specific events drawn from the public record [1], [2].

B. S2 — Reachable Envelope

From the declared specifications the G1 weighs approximately 35 kg with joint torques exceeding 100 N·m [1]. We take a strike-class reach envelope of $L_k = 1.5$ m and note that the distal tip speed of a roundhouse kick is well above 1 m/s—orders of magnitude above any PFL-admissible contact speed, as S3 confirms.

C. S3 — Contact-Limit Allocation and the PFL Verdict

The Urumqi strike landed at adult-abdomen height, which is chest-to-head height on a small child; the governing ISO/TS 15066 limits are therefore the chest and skull/face limits, lower than the 110 N quasi-static / 220 N transient abdominal values and uncertain for pediatric subjects [6], [19]. Evaluating (1) with any plausible effective stiffness and reduced mass for a chest-height contact, the admissible contact speed $v_{\mathrm{rel,max}} = F_{\mathrm{lim}}/\sqrt{k\mu}$ falls well below the tip speed of a deliberate kick. We do not invent the G1's measured kick force, which has not been published [1]; the framework does not require it.

TABLE I
Representative ISO/TS 15066 contact-force limits for body regions reachable by a strike at choreographed adult-abdomen height, which is chest-to-head height for a child. Values per [6]; pediatric applicability unverified per [19].

Region (adult)	**On child**	**Quasi-static**	**Transient**	**PFL for strike?**
Abdomen	Chest	110 N	220 N	No
Chest (sternum)	Neck/face	140 N	280 N	No
Face/skull	Skull	65 N	n/a	No

The structural conclusion is sufficient and certain: a strike-class motion cannot satisfy (1) for the governing body region, so PFL is unavailable and strike-class motion must be lockout-excluded from the bystander-present mode.

D. S4 — Separation Distance

With PFL excluded, we compute the protective separation distance from (2). Using the ISO 13855 walking-approach speed $v_h = 1.6$ m/s [7], an illustrative reaction-plus-stop latency $T_r + T_s = 0.5$ s, the reach $L_k = 1.5$ m, and setting the intrusion and uncertainty terms to zero in this illustrative pass, we obtain $S_p = (1.6)(0.5) + 1.5 = 2.3$ m, which we round up to an enforced 2.5 m barrier offset to absorb the omitted margins. These are illustrative figures, to be replaced by measured stop performance and detection latency before deployment; the point is that the calculation is elementary and that, in the Urumqi event, it was never run. Table I lists the controlling limits and Table II the derived requirements.

E. S5 — Behavior-Policy Gates

G_{sep}: on detection of a bystander inside $S_p = 2.5$ m, the controller initiates a protective stop of all strike-class motion within a bounded latency and transitions to a hold posture below 0.25 m/s. G_{fall}: on fall detection, the controller suppresses commanded joint torque to a safe-flail limit within 100 ms and requires explicit handler re-arm [23], [24]. G_{link}: on detected link degradation or command implausibility, the robot transitions to the MRC within 500 ms, with an independent hardwired emergency-stop channel always available [4], [5].

F. S6 — Fault Tree, Allocation, and Closure

Fig. 2 sketches the fault tree for the top event *bystander struck during public humanoid performance*, with three branches corresponding to the three public-record events [1], [2]. Each branch is an AND-decomposition whose basic events are precisely the requirements that were never written. The protective-stop function on the G_{sep} branch is allocated PL d / category 3 per the ISO 13849-1 risk graph [10]. Table II collects the five derived requirements.

None of these requirements is technologically exotic. PDR-002 is an industrial light curtain expressed in perception software; PDR-004 is the minimum-risk-condition behavior already mandated by the emerging national humanoid standard

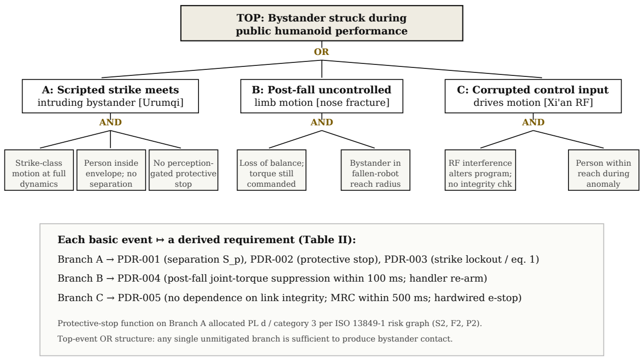

Fig. 2. Fault tree for the top event "Bystander struck during public humanoid performance." The OR gate expands into three branches: A (scripted strike meets intruding bystander, Urumqi), B (post-fall uncontrolled limb motion, nose fracture), and C (corrupted control input, Xi'an). Every basic event corresponds to a derived requirement in Table II.

TABLE II

DERIVED BYSTANDER-SAFETY REQUIREMENTS, EACH TRACED TO A FAULT-TREE BRANCH AND AN ALLOCATED CONTROL. PL PER ISO 13849-1 [10]; CONTACT AND SEPARATION CONTRACTS PER [6], [7].

Req ID	Requirement (abbreviated)	Br.	Alloc.
PDR-001	Enforce separation $\geq S_p$ per (2) (illustrative 2.5 m), validated by measured stop performance	A	ISO 13855; PL d
PDR-002	Protective stop of all strike-class motion on detected intrusion; MRC hold < 0.25 m/s	A	ISO 10218-2; PL d
PDR-003	Lockout-exclude strike-class motion from bystander modes; permitted motion satisfies (1) for child region	A	ISO/TS 15066
PDR-004	On fall, suppress joint torque to safe-flail within 100 ms; require handler re-arm	B	ISO/CD 25785-1; PL d
PDR-005	No dependence on link integrity; MRC within 500 ms; hardwired e-stop always available	C	ISO 10218-2; PL d

system [3]; PDR-005 is two decades of industrial wireless-control practice. What is missing is the *allocation* of that engineering to the public-performance operating mode—exactly the loop the framework closes.

V. Discussion

A. Limitations

The framework is a translation method, not a certification. The correctness of the resulting separation distance and contact-force budget depends entirely on measured inputs—stop time T_s, detection latency T_r, effective stiffness k—that the framework demands but does not supply. The numerical separation distance in Section IV-D is explicitly illustrative; substituting a realistic 1.0 s reaction-plus-stop latency nearly doubles the $v_h(T_r+T_s)$ term and pushes S_p past 3 m. A second limitation is the pediatric-applicability gap: the ISO/TS 15066 limits are preliminary and were not derived for children [19], so Table I should be read as conservative placeholders.

B. Threats to Validity

The principal threat is reliance on press and incident-registry accounts of the 2026 events [1], [2], which lack the instrumented detail of a formal investigation; we therefore avoid any inference that requires a measured contact force and ground the central S3 verdict in the structural impossibility of PFL-compliant strikes, which holds independent of the specific force value. A second threat is scope transfer: ISO 10218 and ISO/TS 15066 are industrial-robot standards [4]–[6], and applying their vocabulary to a performance humanoid is an argument by analogy until ISO/CD 25785-1 is published [11]. We regard the transfer as defensible because the hazard—a torque-dense articulated machine contacting a human—is the same hazard the industrial standards were written to control.

C. Where the Standards Lens Stops

Two dimensions lie beyond the framework. First, the behavior policies driving modern humanoids are increasingly learned and may be non-deterministic; a safety case built on a fixed motion library does not bound a policy that can generate novel motions, and the Xi'an interference event [2] hints at how brittle the mapping from intended to executed behavior can be. Run-time control-barrier-function enforcement [22] partially addresses this, but assurance of the learned policy itself is an open problem no current robotic-safety standard closes. Second, as Salvini *et al.* argue, public space introduces crowd dynamics, social-proxemic expectations, and human misbehavior that EN ISO 13482 does not capture [25]; a separation distance enforced against a single approaching pedestrian does not generalize cleanly to a dense, mobile crowd of children. The framework is the deterministic floor of a public-deployment safety case, not its ceiling.

VI. Conclusion and Future Work

A cluster of bystander-contact events involving untethered humanoid robots in public demonstrations during the first half of 2026 exposed a gap that is not a gap in technology but a gap in allocation: the safeguarding methods of ISO 10218-2, ISO/TS 15066, and ISO 13855 are mature, yet none had been applied to the public-performance operating mode in which the incidents occurred. We presented a six-step cross-standards framework that closes the loop from a contact incident to a verifiable, mode-gated requirement set, formalized two contracts, and demonstrated the framework end-to-end on the Unitree G1 cluster, deriving five traceable requirements with an allocated PL d protective-stop function.

Future work proceeds along three lines. The first is empirical: a measured database of humanoid contact forces and stop times, including pediatric-relevant biomechanical limits, would replace the illustrative inputs of Section IV with validated ones. The second is methodological: extending the framework's deterministic gates with assurance arguments for learned behavior policies, coupling a run-time control-barrier-function layer to a claim-based safety case. The third is regulatory: as ISO/CD 25785-1 and the emerging national humanoid standard systems move toward publication [3], [11], the framework offers a template for the public-performance clauses those standards will need.

References

[1] Interesting Engineering, "Viral: Humanoid robot kicks child in stomach during public demonstration in China," *Interesting Eng.*, Jun. 5, 2026. [Online]. Available: https://interestingengineering.com/ai-robotics/viral-humanoid-robot-kicks-child-in-stomach

[2] OECD, "Robot malfunction at Chinese university event leads to unintended physical contact," *OECD.AI Incidents Monitor*, incident 2026-04-24-9951, Apr. 24, 2026. [Online]. Available: https://oecd.ai/en/incidents/2026-04-24-9951

[3] Robotics and Automation News, "Why China's new humanoid robot standards could change the industry," Mar. 31, 2026. [Online]. Available: https://roboticsandautomationnews.com/2026/03/31/why-chinas-new-humanoid-robot-standards-could-change-the-industry/100263/

[4] ISO, *ISO 10218-1:2025 Robotics — Safety requirements — Part 1: Industrial robots*, ISO, Geneva, 2025.

[5] ISO, *ISO 10218-2:2025 Robotics — Safety requirements — Part 2: Industrial robot applications and robot cells*, ISO, Geneva, 2025.

[6] ISO, *ISO/TS 15066:2016 Robots and robotic devices — Collaborative robots*, ISO, Geneva, 2016.

[7] ISO, *ISO 13855:2024 Safety of machinery — Positioning of safeguards with respect to the approach of the human body*, ISO, Geneva, 2024.

[8] ISO, *ISO 13482:2014 Robots and robotic devices — Safety requirements for personal care robots*, ISO, Geneva, 2014.

[9] ISO, *ISO 12100:2010 Safety of machinery — General principles for design — Risk assessment and risk reduction*, ISO, Geneva, 2010.

[10] ISO, *ISO 13849-1:2023 Safety of machinery — Safety-related parts of control systems — Part 1: General principles for design*, ISO, Geneva, 2023.

[11] ISO, *ISO/CD 25785-1 Robotics — Safety requirements for industrial mobile robots with actively controlled stability — Part 1: Robots*, ISO, Geneva, committee draft, 2026.

[12] S. Haddadin, A. De Luca, and A. Albu-Schäffer, "Robot collisions: a survey on detection, isolation, and identification," *IEEE Trans. Robot.*, vol. 33, no. 6, pp. 1292–1312, Dec. 2017, doi: 10.1109/TRO.2017.2723903.

[13] A. De Santis, B. Siciliano, A. De Luca, and A. Bicchi, "An atlas of physical human–robot interaction," *Mech. Mach. Theory*, vol. 43, no. 3, pp. 253–270, Mar. 2008, doi: 10.1016/j.mechmachtheory.2007.03.003.

[14] A. Bicchi and G. Tonietti, "Fast and 'soft-arm' tactics: dealing with the safety-performance tradeoff in robot arms design and control," *IEEE Robot. Autom. Mag.*, vol. 11, no. 2, pp. 22–33, Jun. 2004, doi: 10.1109/MRA.2004.1310939.

[15] J. A. Marvel and R. Norcross, "Implementing speed and separation monitoring in collaborative robot workcells," *Robot. Comput.-Integr. Manuf.*, vol. 44, pp. 144–155, Apr. 2017, doi: 10.1016/j.rcim.2016.08.001.

[16] C. Byner, B. Matthias, and H. Ding, "Dynamic speed and separation monitoring for collaborative robot applications — concepts and performance," *Robot. Comput.-Integr. Manuf.*, vol. 58, pp. 239–252, Aug. 2019, doi: 10.1016/j.rcim.2018.11.002.

[17] N. Lucci, B. Lacevic, A. M. Zanchettin, and P. Rocco, "Combining speed and separation monitoring with power and force limiting for safe collaborative robotics applications," *IEEE Robot. Autom. Lett.*, vol. 5, no. 4, pp. 6121–6128, Oct. 2020, doi: 10.1109/LRA.2020.3010211.

[18] A. M. Zanchettin, N. M. Ceriani, P. Rocco, H. Ding, and B. Matthias, "Safety in human-robot collaborative manufacturing environments: metrics and control," *IEEE Trans. Autom. Sci. Eng.*, vol. 13, no. 2, pp. 882–893, Apr. 2016, doi: 10.1109/TASE.2015.2412256.

[19] R. Behrens, G. Pliske, M. Umbreit, S. Piatek, F. Walcher, and N. Elkmann, "A statistical model to determine biomechanical limits for physically safe interactions with collaborative robots," *Front. Robot. AI*, vol. 8, art. 667818, Feb. 2022, doi: 10.3389/frobt.2021.667818.

[20] M. Rosenstrauch and J. Krüger, "Safe human-robot-collaboration — introduction and experiment using ISO/TS 15066," in *Proc. 3rd Int. Conf. Control, Autom. Robot. (ICCAR)*, 2017, pp. 740–744, doi: 10.1109/ICCAR.2017.7942795.

[21] L. Scalera, C. Nainer, A. Giusti, and A. Gasparetto, "Robust safety zones for manipulators with uncertain dynamics in collaborative robotics," *Int. J. Comput. Integr. Manuf.*, vol. 37, no. 9, Sep. 2023, doi: 10.1080/0951192X.2023.2258111.

[22] F. Ferraguti, C. T. Landi, S. Costi, M. Bonfè, S. Farsoni, C. Secchi, and C. Fantuzzi, "Safety barrier functions and multi-camera tracking for human–robot shared environment," *Robot. Auton. Syst.*, vol. 124, art. 103388, Feb. 2020, doi: 10.1016/j.robot.2019.103388.

[23] R. Subburaman, D. Kanoulas, N. Tsagarakis, and J. Lee, "A survey on control of humanoid fall over," *Robot. Auton. Syst.*, vol. 166, art. 104443, Aug. 2023, doi: 10.1016/j.robot.2023.104443.

[24] Q. Li, X. Chen, Y. Zhou, Z. Yu, W. Zhang, and Q. Huang, "A minimized falling damage method for humanoid robots," *Int. J. Adv. Robot. Syst.*, vol. 14, no. 5, Sep. 2017, doi: 10.1177/1729881417728016.

[25] P. Salvini, D. Paez-Granados, and A. Billard, "On the safety of mobile robots serving in public spaces: identifying gaps in EN ISO 13482:2014 and calling for a new standard," *ACM Trans. Hum.-Robot Interact.*, vol. 10, no. 3, art. 19, Jul. 2021, doi: 10.1145/3442678.

[26] Y. Zhang, J. Wang, and L. Chen, "Dynamic speed and separation monitoring for human-robot collaboration based on binocular vision," *J. Intell. Robot. Syst.*, vol. 111, art. 38, Mar. 2025, doi: 10.1007/s10846-025-02268-7.

[27] ASTM International, "ASTM calls for urgent safety standards for humanoid robots (subcommittee F45.06 on legged robots)," *TechJournal*, Sep. 13, 2025. [Online]. Available: https://www.techjournal.uk/p/astm-calls-for-urgent-safety-standards